F_2 and F_L at small x using a collinearly improved BFKL resummation

Martin Hentschinski,[1] Agustín Sabio Vera,[2] and Clara Salas[2]

[1]*Physics Department, Brookhaven National Laboratory, Upton, New York 11973, USA*
[2]*Instituto de Fsica Teórica UAM/CSIC and Universidad Autónoma de Madrid, E-28049 Madrid, Spain*

We present a detailed description of the Q^2 and x dependence of the structure functions F_2 and F_L as extracted from the deep inelastic scattering data at HERA in the small Bjorken x region. Making use of a collinearly improved Balitsky-Fadin-Kuraev-Lipatov equation at next-to-leading order and a treatment of the running of the coupling using non-Abelian physical renormalization together with the Brodsky-Lepage-Mackenzie scale choice allows us to reach low values of Q^2. We also provide some predictions for future lepton-hadron colliders.

I. INTRODUCTION AND REVIEW OF OUR FRAMEWORK

Recently, in Ref. [1], we calculated the effective slope λ for the structure function F_2 when parameterized as $\sim x^{-\lambda}$ at low Bjorken x, which ranges from $\lambda \simeq 0.1$ to $\simeq 0.3$ when moving from low to high values of Q^2. The importance of a correct understanding of the HERA data using perturbative QCD techniques, in particular for the physics program at the Large Hadron Collider (LHC), has been largely discussed in the literature (see, e.g., Ref. [2]).

In this paper we will not only further investigate the Q^2 and x dependence of F_2 but also study in detail the longitudinal structure function F_L. As in Ref. [1] we will explore the small x region using the next-to-leading order (NLO) [3] Balitsky-Fadin-Kuraev-Lipatov (BFKL) [4] equation with collinear improvements, together with optimal renormalization schemes.

Let us first briefly review our formulas [1]. At small $x \simeq Q^2/s$, with s being the squared center-of-mass energy, we can apply high energy factorization [5] and write the structure functions F_I, $I = 2, L$ as (note that the integrations take place in the transverse space with $q \equiv \sqrt{\mathbf{q}_\perp^2}$)

$$F_I(x, Q^2) = \int \frac{d^2\mathbf{q}_\perp}{\pi q^2} \int \frac{d^2\mathbf{p}_\perp}{\pi p^2} \Phi_I(q, Q^2) \Phi_P(p, Q_0^2) \mathcal{F}(x, q, p).$$

(1)

Φ_P is the nonperturbative proton impact factor which we model using

$$\Phi_P(p, Q_0^2) = \frac{\mathcal{C}}{\Gamma(\delta)} \left(\frac{p^2}{Q_0^2}\right)^\delta e^{-\frac{p^2}{Q_0^2}},$$

(2)

where we have introduced two free parameters and a normalization. Φ_I is the impact factor associated to the photon which in Ref. [1] we treated at leading-order (LO), i.e.,

$$\int \frac{d^2\mathbf{q}_\perp}{\pi q^2} \Phi_I(q, Q^2) \left(\frac{q^2}{Q^2}\right)^{\gamma - 1} = \frac{\alpha_s(\mu^2)}{2\pi} \sum_{q=1}^{n_f} e_q^2 c_I(\nu),$$

(3)

where

$$c_I(\nu) \equiv \frac{\pi^2}{4} \frac{\Omega_I(\nu)}{(\nu + \nu^3)} \operatorname{sech}(\pi\nu) \tanh(\pi\nu),$$

(4)

$\nu = i(1/2 - \gamma)$, $\Omega_2 = (11 + 12\nu^2)/8$, $\Omega_L = \nu^2 + 1/4$, and the strong coupling α_s is fixed at the renormalization scale μ^2. In the present work we will also use the kinematically improved impact factors proposed in Refs. [6,7], which include part of the higher order corrections by considering exact gluon kinematics. Its implementation requires one to replace the functions $c_I(\nu)$ by $\tilde{c}_I(\gamma, \omega)$, where

$$\tilde{c}_L(\gamma, \omega) = \frac{4\Gamma(\gamma + \xi + 1)\Gamma(1 + \gamma)[(\psi(\gamma + \xi) - \psi(\gamma))(3\omega^2 - \xi^2 + 1) - 6\omega\xi]}{\xi\Gamma(1 + \omega)(\xi^4 - 5\xi^2 + 4)}$$

(5)

and $\tilde{c}_2 = \tilde{c}_L + \tilde{c}_T$, with

$$\tilde{c}_T(\gamma, \omega) = \frac{\Gamma(\gamma + \xi)\Gamma(\gamma)}{\xi\Gamma(1 + \omega)(\xi^4 - 5\xi^2 + 4)} \{-2\xi\omega(\xi^2 + 3^2 + 6\omega + 11) + [\psi(\gamma + \xi) - \psi(\gamma)]$$
$$\times [\xi^4 - 10\xi^2 + 3\omega^2(\omega^2 + 2\omega + 4) - 2\omega(\xi^2 - 1) + 9]\}.$$

(6)

$\psi(\gamma)$ is the logarithmic derivative of the Euler Gamma function and $\xi = 1 - 2\gamma + \omega$, while ω is the Mellin variable conjugate to x in the definition of the gluon Green function $\mathcal{F}$; see Eq. (7) below. The main difference between these impact factors is that the LO ones roughly double the value of their kinematically improved counterparts in the region with small $|\nu|$, while being very similar for $|\nu| \gtrsim 1$.

The gluon Green function can be written in the form

$$\mathcal{F}(x, q, p) = \frac{1}{\pi} \int \frac{d\omega}{2\pi i} \int \frac{d\gamma}{2\pi i} \ \frac{1}{q^2} \left(\frac{q^2}{p^2}\right)^{\gamma} x^{-\omega} \frac{1}{\omega - \bar{\alpha}_s \hat{\mathcal{K}}(\gamma)}, \tag{7}$$

with $\bar{\alpha}_s = \alpha_s N_c / \pi$. The collinearly improved BFKL kernel as introduced in Eq. (7) is an operator consisting of a diagonal (scale invariant) piece $\hat{\chi}(\gamma)$ with eigenvalue

$$\chi(\gamma) = \bar{\alpha}_s \chi_0(\gamma) + \bar{\alpha}_s^2 \chi_1(\gamma) - \frac{1}{2} \bar{\alpha}_s^2 \chi_0'(\gamma) \chi_0(\gamma) + \chi_{\mathrm{RG}}(\bar{\alpha}_s, \gamma, a, b), \tag{8}$$

where $\chi_0(\gamma) = 2\psi(1) - \psi(\gamma) - \psi(1 - \gamma)$, $a = \frac{5}{12} \times \frac{\beta_0}{N_c} - \frac{13}{36} \frac{n_f}{N_c^3} - \frac{55}{36}$ and $b = -\frac{1}{8} \frac{\beta_0}{N_c} - \frac{n_f}{6N_c^3} - \frac{11}{12}$, plus a term $\hat{\chi}_{\mathrm{RC}}(\gamma)$ proportional to β_0 which contains the running coupling corrections of the NLO kernel [8]:

$$\hat{\chi}_{\mathrm{RC}}(\gamma) = \bar{\alpha}_s^2 \frac{\beta_0}{8N_c} (\chi_0(\gamma)\vec{\partial}_\gamma - \overleftarrow{\partial}_\gamma \chi_0(\gamma) + 2\log(\mu^2)). \tag{9}$$

The precise form of the NLO kernel χ_1 can be found in Ref. [1]. The resummation of collinear logarithms of order $\bar{\alpha}_s^3$ and beyond is realized by the term [1,9,10]

$$\chi_{\mathrm{RG}}(\bar{\alpha}_s, \gamma, a, b) = \bar{\alpha}_s(1 + a\bar{\alpha}_s)(\psi(\gamma) - \psi(\gamma - b\bar{\alpha}_s)) - \frac{\bar{\alpha}_s^2}{2} \psi''(1 - \gamma) - b\bar{\alpha}_s^2 \frac{\pi^2}{\sin^2(\pi\gamma)}$$

$$+ \frac{1}{2} \sum_{m=0}^{\infty} \left(\gamma - 1 - m + b\bar{\alpha}_s - \frac{2\bar{\alpha}_s(1 + a\bar{\alpha}_s)}{1 - \gamma + m} + \sqrt{(\gamma - 1 - m + b\bar{\alpha}_s)^2 + 4\bar{\alpha}_s(1 + a\bar{\alpha}_s)}\right). \tag{10}$$

Our final expression for the structure functions reads

$$F_I(x, Q^2) \propto \int d\nu \, x^{-\chi(\frac{1}{2}+i\nu)} \Gamma\left(\delta - \frac{1}{2} - i\nu\right)\left[1 + \frac{\bar{\alpha}_s^2 \beta_0 \chi_0(\frac{1}{2}+i\nu)}{8N_c} \log\left(\frac{1}{x}\right)\right.$$

$$\left. \times \left(i(\pi\coth(\pi\nu) - 2\pi\tanh(\pi\nu) - M_I(\nu)) - \psi\left(\delta - \frac{1}{2} - i\nu\right)\right)\right]\left(\frac{Q^2}{Q_0^2}\right)^{\frac{1}{2}+i\nu} c_I(\nu), \tag{11}$$

where M_2 and M_L can be found in Ref. [1]. For the kinematical improved version of F_I we replace $c_I(\nu)$ by $\tilde{c}_I(1/2 + i\nu, \chi(1/2 + i\nu))$.

In Eq. (11) the scale of the running of the coupling has been set to $\mu^2 = QQ_0$. Building on the work of Ref. [11] we found in Ref. [1] that in order to obtain a good description of the Q^2 dependence of the effective intercept of F_2, λ, for $x < 10^{-2}$, it is very useful to operate with non-Abelian physical renormalization schemes using the Brodsky-Lepage-Mackenzie optimal scale setting [12] with the momentum space physical renormalization scheme [13]. For technical details on our precise implementation we refer the reader to Ref. [1] (see also Ref. [14] for a review on the subject and [15] for a related work). More qualitatively, in these schemes the pieces of the NLO BFKL kernel proportional to β_0 are absorbed in a new definition of the running coupling in order to remove the infrared renormalon ambiguity. Once this is done, the residual scheme dependence in this framework is very small. We also found it convenient [1] to introduce, in order to describe the data with small Q^2, an analytic parametrization of the running coupling in the infrared proposed in Ref. [16].

II. COMPARISON TO DEEP INELASTIC SCATTERING EXPERIMENTAL DATA

In the following we compare our results with the experimental data for F_2 and F_L.
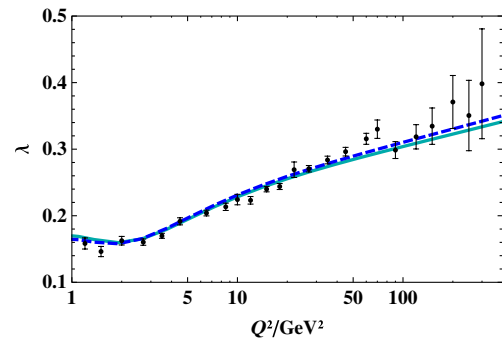

FIG. 1 (color online). Fit to λ for F_2 with the LO photon impact factor (solid line) and the kinematically improved one (dashed line). The data set has been extracted from Ref. [17].

A. F_2

Let us first compare the result obtained in Ref. [1] for the logarithmic derivative $d\log F_2/d\log(1/x)$ using Eq. (11) with a LO photon impact factor and our new calculation using the kinematically improved one. In Fig. 1 we present our results with the values of our best fits for both types of impact factors and compare them with the H1-ZEUS combined data [17] for $x < 10^{-2}$. The values of the parameters defining the proton impact factor in (2) and the position

of the (regularized) Landau pole (we use $n_f = 4$) for the strong coupling are $\delta = 8.4$, $Q_0 = 0.28\,\text{GeV}$, $\Lambda = 0.21$ GeV for the LO order case and $\delta = 6.5$, $Q_0 = 0.28$ GeV, $\Lambda = 0.21$ GeV for the kinematically improved (note that the normalization $\mathcal{C}$ does not contribute to this quantity).

The LO impact factor generates lower values than the kinematically improved one in the high Q^2 region and slightly higher ones when $Q^2 \lesssim 2$ GeV^2. It is interesting to see how the approach presented here allows for a good
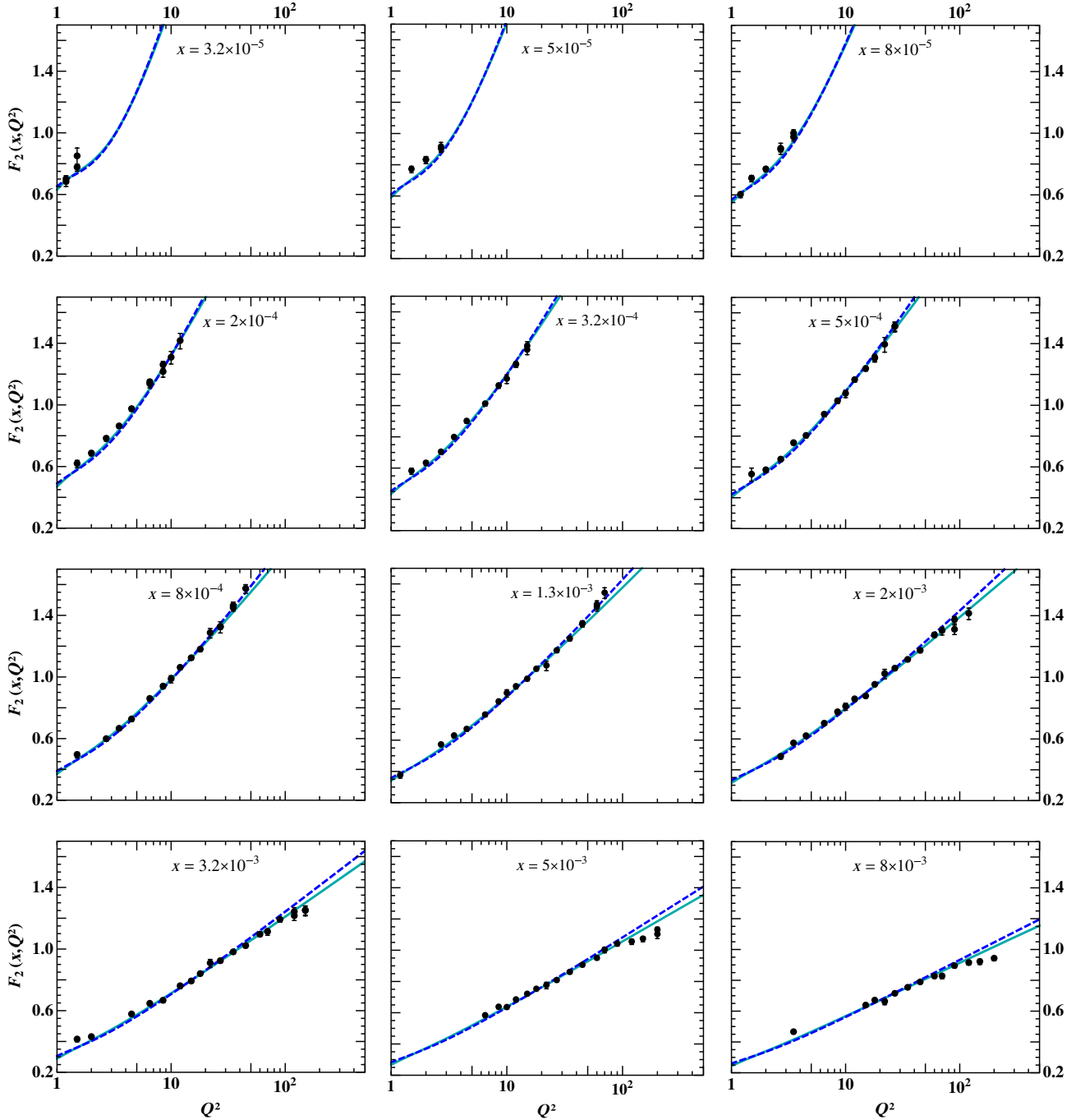

FIG. 2 (color online). Study of the dependence of $F_2(x, Q^2)$ on Q^2 using the LO photon impact factor (solid lines) and the kinematically improved one (dashed lines). Q^2 runs from 1.2 to 200 GeV^2.

description of the data in a very wide range of Q^2, not only for high values, where the experimental uncertainties are larger, but also in the nonperturbative regions due to our treatment of the running of the coupling.

Encouraged by these positive results we now turn to investigate more differential distributions. We select data with fixed values of x and compare the Q^2 dependence of our theoretical predictions with them, now fixing the normalization for the LO impact factor to $\mathcal{C} = 1.50$ and 2.39 for the kinematically improved. Our results are presented in Fig. 2. The equivalent comparison to data, this time

fixing Q^2 and looking into the evolution in the x variable, is shown in Fig. 3. We observe that our predictions give a very accurate description of the data (the typical chi-square per degree of freedom is, e.g., 1.2 in the region with Q^2 from 4.5 to 120 GeV^2) for both types of impact factors.

Let us remark that the values for the parameters in this fit are in syntony with the theoretical expectations for the proton impact factor since Q_0 is very similar to the confinement scale and the value of δ sets the maximal contribution from the impact factor also in that region. This is reasonable given that the proton has a large transverse size.
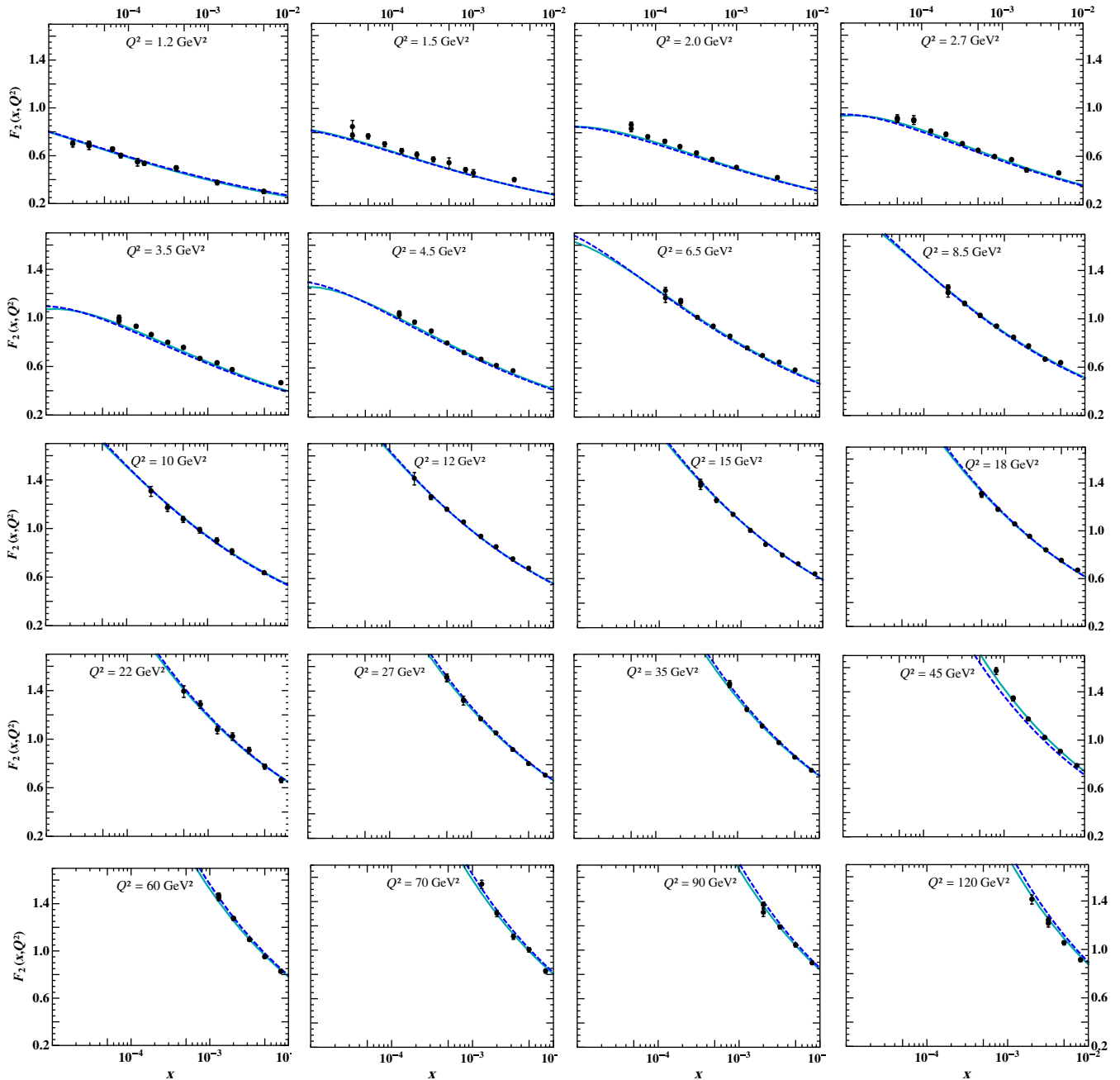

FIG. 3 (color online). Study of the dependence of $F_2(x, Q^2)$ on x using the LO photon impact factor (solid lines) and the kinematically improved one (dashed lines). Q^2 runs from 1.2 to 120 GeV^2.
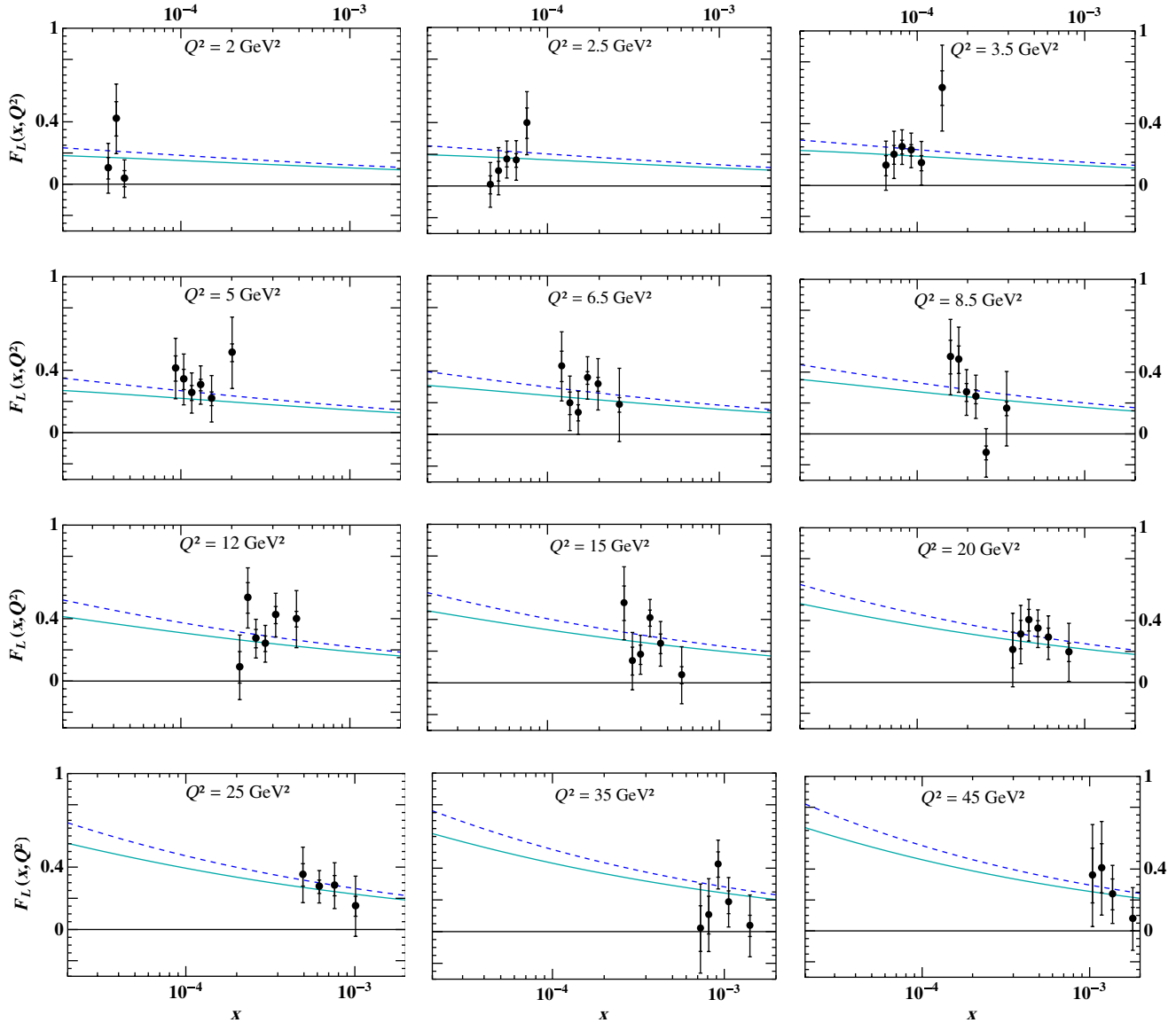
FIG. 4 (color online).   Fit to F_L with the LO photon impact factor (solid lines) and the improved one (dashed lines). The experimental data are taken from Ref. [18].

B. F_L

The longitudinal structure function is an interesting observable which is very sensitive to the gluon content of the proton. We will now present our predictions for F_L using the best values for the parameters previously obtained in the fit of F_2. We will see that the agreement with the data is very good. First, Q^2 is fixed and the x dependence is investigated in Fig. 4. The experimental data have been taken from Ref. [18]. To present the Q^2 dependence it is convenient to calculate, for each bin in Q^2, the average value of x; see Fig. 5. In some sense this is a similar plot to the one previously presented for λ in the F_2 analysis and we can see that the effect of using different types of impact factors is to generate a global shift in the normalization. Again we note that we have an accurate description of the
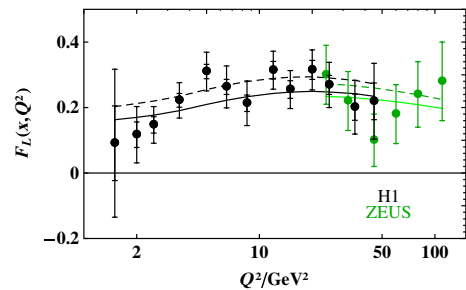

FIG. 5 (color online).   The proton structure function F_L as a function of Q^2. The average x values for each Q^2 of the H1 data (black) are given in Fig. 13 of Ref. [18]. ZEUS data are taken from Ref. [20]. The solid line represents our calculation with the LO photon impact factor and the dashed line using the kinematically improved one.
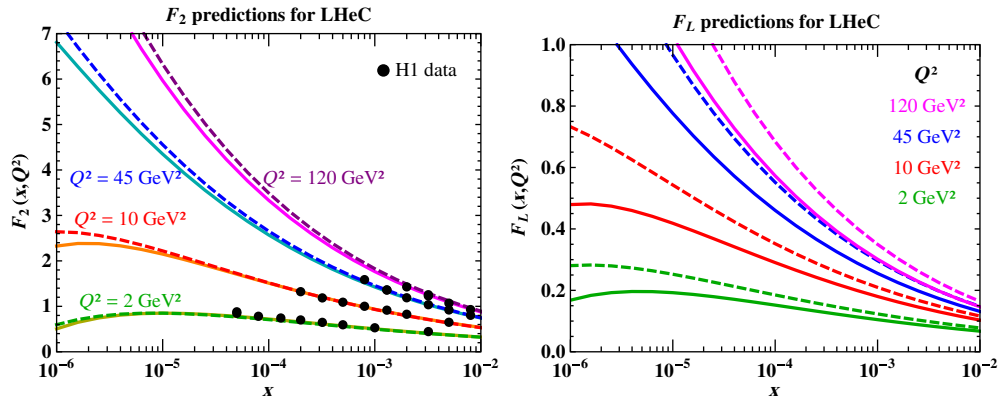
FIG. 6 (color online). Predictions for F_2 (left) and F_L (right) for LHeC. On the left plot, the curve with $Q^2 = 10$ GeV^2 can be compared with Fig. 4.13 of Ref. [22]. Simulated measurements for F_L in the kinematic range plotted here (right) can be found in Fig. 3.7 of the same reference.

transition from high to low Q^2, which was one of the main targets of our work.

III. PREDICTIONS FOR FUTURE COLLIDERS

While our predictions for the structure functions are in agreement with the data from the HERA collider experiments H1 and ZEUS, these observables are too inclusive to provide unambiguous evidence for BFKL evolution (for other recent studies in this context see Ref. [19]). Comparable in quality fits can be obtained by both Dokshitzer-Gribov-Lipatov-Altarelli-Parisi evolution and saturation models; see, e.g., Refs. [18,20]. In order to distinguish among different parton evolution pictures new collider experiments are needed, such as the proposed Electron-Ion-Collider at BNL/JLab (USA) [21] and the Large Hadron Electron Collider (LHeC) at CERN (Switzerland) [22], which will be able to measure both F_2 and F_L at unprecedented small values of Bjorken x. In Fig. 6 we present two studies with our predictions for F_2 and F_L down to values of $x = 10^{-6}$.

IV. CONCLUSIONS

We have presented an application of the BFKL resummation program to the description of the x and Q^2 dependence of structure functions as extracted from deep inelastic scattering data at HERA. We have also provided some predictions for these observables at future colliders. In order to obtain the correct dependence on the virtuality of the photon at high values of the scattering energy, we have included in the BFKL kernel the main collinear contributions to all orders. We have also used optimal renormalization and an analytic running coupling in the infrared in order to accurately describe the regions of low Q^2. Our next task will be to use these parameterizations to describe more exclusive observables, such as heavy quark and multijet production, at the Large Hadron Collider at CERN.

[1] M. Hentschinski, A. S. Vera, and C. Salas, Phys. Rev. Lett. **110,** 041601 (2013).

[2] M. Dobbs *et al.*, arXiv:hep-ph/0403100; M. Dittmar *et al.*, arXiv:hep-ph/0511119; S. Alekhin *et al.*, arXiv:hep-ph/0601012; J. R. Andersen *et al.* (Small x Collaboration), Eur. Phys. J. C **48,** 53 (2006); H. Jung *et al.*, arXiv:0809.0549; Z. J. Ajaltouni *et al.*, arXiv:0903.3861.

[3] V. S. Fadin and L. N. Lipatov, Phys. Lett. B **429,** 127 (1998); M. Ciafaloni and G. Camici, Phys. Lett. B **430,** 349 (1998).

[4] L. N. Lipatov, Sov. J. Nucl. Phys. **23,** 338 (1976); E. A. Kuraev, L. N. Lipatov, and V. S. Fadin, Phys. Lett. **60B,** 50 (1975); Sov. Phys. JETP **44,** 443 (1976); **45,** 199 (1977); I. I. Balitsky and L. N. Lipatov, Sov. J. Nucl. Phys. **28,** 822 (1978).

[5] J. R. Forshaw and D. A. Ross, Lect. Notes Phys. **9,** 1 (1997).

[6] J. Kwiecinski, A. D. Martin, and A. M. Stasto, Phys. Rev. D **56**, 3991 (1997).

[7] A. Bialas, H. Navelet, and R. B. Peschanski, Nucl. Phys. **B603**, 218 (2001).

[8] A. S. Vera and F. Schwennsen, Phys. Rev. D **77**, 014001 (2008); Nucl. Phys. **B776**, 170 (2007); A. S. Vera, Nucl. Phys. **B746**, 1 (2006); F. Caporale, A. Papa, and A. S. Vera, Eur. Phys. J. C **53**, 525 (2008).

[9] G. P. Salam, J. High Energy Phys. 07 (1998) 019.

[10] A. S. Vera, Nucl. Phys. **B722**, 65 (2005).

[11] S. J. Brodsky, V. S. Fadin, V. T. Kim, L. N. Lipatov, and G. B. Pivovarov, JETP Lett. **70**, 155 (1999); Pis'ma Zh. Eksp. Teor. Fiz. **76**, 306 (2002) [JETP Lett. **76**, 249 (2002)].

[12] S. J. Brodsky, G. P. Lepage, and P. B. Mackenzie, Phys. Rev. D **28**, 228 (1983).

[13] W. Celmaster and R. J. Gonsalves, Phys. Rev. D **20**, 1420 (1979); Phys. Rev. Lett. **42**, 1435 (1979); P. Pascual and R. Tarrach, Nucl. Phys. **B174**, 123 (1980); **B181**, 546 (1981).

[14] S. J. Brodsky and L. Di Giustino, Phys. Rev. D **86**, 085026 (2012).

[15] M. Angioni, G. Chachamis, J. D. Madrigal, and A. S. Vera, Phys. Rev. Lett. **107**, 191601 (2011).

[16] B. R. Webber, J. High Energy Phys. 10 (1998) 012.

[17] F. D. Aaron *et al.* (H1 and ZEUS Collaboration), J. High Energy Phys. 01 (2010) 109.

[18] F. D. Aaron *et al.* (H1 Collaboration), Eur. Phys. J. C **71**, 1579 (2011).

[19] H. Kowalski, L. N. Lipatov, D. A. Ross, and G. Watt, Eur. Phys. J. C **70**, 983 (2010); H. Kowalski, L. N. Lipatov, and D. A. Ross, arXiv:1109.0432; arXiv:1205.6713.

[20] S. Chekanov *et al.* (ZEUS Collaboration), Phys. Lett. B **682**, 8 (2009).

[21] A. Deshpande *et al.*, arXiv:1212.1701; D. Boer *et al.*, arXiv:1108.1713.

[22] J. L. Abelleira Fernandez *et al.* (LHeC Study Group Collaboration), J. Phys. G **39**, 075001 (2012).